

Bond Strength of Rectangular CFSST Columns after Exposed to Elevated Temperature

Anandapadmanaban K.¹ , A. S. Santhi^{1*} 

¹ School of Civil Engineering, Vellore Institute of Technology Vellore-632014, India.

Received 21 September 2023; Revised 14 February 2024; Accepted 20 February 2024; Published 01 March 2024

Abstract

This article investigates the bond-behavior of Rectangular Concrete-filled stainless-steel tubular (RCFSST) columns under post-fire conditions. The main objective of this research was to obtain τ -s relationship of RCFSST columns under the combined effects of high temperature and concrete age. A total of sixteen specimens, including four reference specimens, were tested with different parameters, namely: i) temperature (600 °C, 800 °C & 1000 °C) ii) different concrete ages (30 days, 60 days, 90 days & 180 days). Analyzing the τ -s curves of the test specimens, chemical adhesion and micro-locking were the principal forces contributing to bond strength at lower concrete ages under post-fire conditions. At a higher concrete age, RCFSST specimens displayed a longer curve after the inflection point, indicating the contribution of macro-locking forces in amplifying the bond-strength. Five distinct curve types were found from the experiments. Type 1 curves with three stages, i) initial linear, ii) non-linear, and ii) final linear stage, had a higher frequency among the other types. For 90-day cured specimens, a decline in bond strength was observed at higher temperatures, but for 180 days cured specimens, a significant rise was seen under post-fire conditions. A new set of τ -s relations for RCFSST columns with different concrete ages under post-fire was established.

Keywords: Bond-Behaviour; Rectangle Stainless-Steel; Concrete Age; Concrete-Filled Stainless-Steel Tubular Columns; Push-Out Test.

1. Introduction

In the context of innovative composite structures, concrete-filled stainless-steel tubular (CFSST) columns contribute more beneficial features in the construction field. The merits of encasing concrete with steel tubes perform better in most of the complex loading conditions. Higher ductility and energy dissipation characteristics [1], competence in seismic zones [1], higher static load resisting capacity, and transverse impact resistance capabilities [2] make these structures an inevitable choice among engineers. Currently, there is a demand for the performance of these structures under various fire scenarios. With these rises in demand, research on exploring new probabilities for enhancing the fire performance of these structures is being carried out.

One of the most crucial features that needs to be optimized in these situations is the bond between steel and concrete. The bond between the inner side of the steel tube and the core concrete plays a vital role in developing a composite action. Without sufficient bond development, the concrete core and stainless-steel act as individual elements, supporting the load disjointedly. Generally, the bond between the inner part of the steel tube and the outer surface of the core concrete takes place through interface frictional forces between the steel and concrete surface, chemical adhesive forces, and mechanical interlock forces [3], as shown in Figure 1. The interface friction force between stainless steel and concrete provides a major contribution to the shear resistance, whereas significant contributions were also noted from

* Corresponding author: as_santhi@vit.ac.in

 <http://dx.doi.org/10.28991/CEJ-2024-010-03-019>



© 2024 by the authors. Licensee C.E.J, Tehran, Iran. This article is an open access article distributed under the terms and conditions of the Creative Commons Attribution (CC-BY) license (<http://creativecommons.org/licenses/by/4.0/>).

the chemical adhesive force and the mechanical interlock forces [3]. Figure 2 shows the ideal response of the CFST column under the push-out test [4]. Various factors influence the bond between the inner tube and concrete infill in CFSST columns. The factors include steel tube thickness, concrete shrinkage, type of aggregates, temperature in core concrete, shape of the sections [5], and surface roughness.

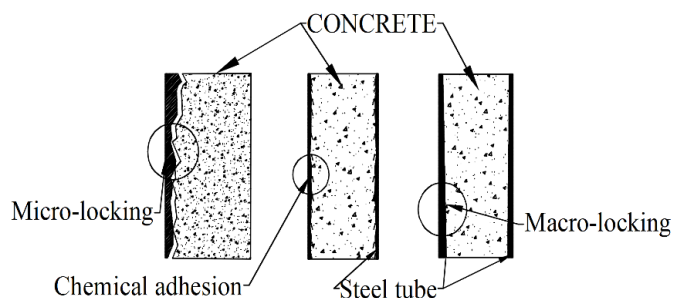


Figure 1. Illustration of various bond mechanism in CFST columns

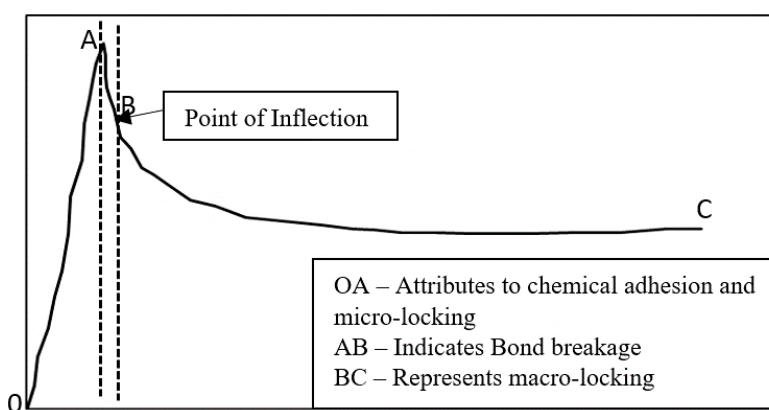


Figure 2. Ideal τ -s curve of CFST columns

Circular CFST sections have more advanced bond strength than other sections. Hoop stresses developed in circular sections increase the confinement of concrete, resulting in higher bond strength. Rectangular and square sections have lower bond strengths. This is due to the fact that the corner regions of rectangular and square sections are ineffective in bonding and reduce bonding capacity. In rectangular CFST columns, the major contribution to the bond strength was governed by the macro-locking mechanism. The influence of friction and chemical adhesion was less significant [6].

Steel tubes with smooth inner surfaces reduce friction between the inner surface and concrete, resulting in a reduction in bond strength [5]. Concrete with light-weight aggregate demonstrates higher bond strength when compared to normal aggregates [7]. A series of tests on the bond strength of steel-encased concrete and concrete-encased steel composite columns were conducted with normal and ultra-high-performance concrete (UHPC) [8]. Concrete-encased steel columns with both normal and UHPC concrete displayed a significant increase in bond strength compared to steel-encased concrete columns. A series of tests were conducted by embedding reinforcing bars in UHPC concrete in CFST columns, and a simplified local bond-slip model was proposed [9]. Test variables include anchorage length ($2d$, $5d$, $7d$), where d is the diameter of the embedded bar. For anchorage lengths less than twice the diameter of the bar, a uniform bond-stress distribution was observed during pull-out tests. Whereas, for anchorage length less than $7d$, a linear distribution of bond stress was observed.

Concrete shrinkage is also an important factor that affects the bond strength, and measures have been taken to reduce shrinkage by replacing normal concrete with expansive concrete, which exhibited better results [5]. The age of concrete increases the shrinkage effects. For longer-lasting concrete, the steel type had a lesser influence on bond strength [5]. Special provisions such as welding internal rings and shear studs were employed to increase the bond capacity of composite sections, and welding internal rings showed enhanced bond strength [10]. Post-fire test results show a clear contribution of shape effects and temperature effects on the bond strength of CFST columns [11]. However, in square columns, an increase in bond strength was absorbed after exposing the specimens for up to 180 minutes after initial decrement. This was explained by the thermal expansion of the concrete core, resulting in an increase in frictional resistance between steel and concrete surfaces. Four different types of curves were categorized [5] for carbon steel,

stainless steel, circular, and square cross-sections, namely Type A, Type B, Type-C, and Type-D curves, as shown in Figure 3. Type A curve has an early linear segment, following a non-linear curve before reaching the peak point, beyond which bond stress reduces gradually. Carbon steel specimens exhibited a Type A response. Type B exhibited a similar trend as in Type A, but in the post-peak stage, a significant drop in bond stress was observed, followed by a recovery in bond stress. Stainless steel exhibited a Type B response. Types C and D had an initial linear portion as well, but their curves tend to have an upper trail during the entire loading stage. Type C and Type D responses were observed in the post-fire push-out test.

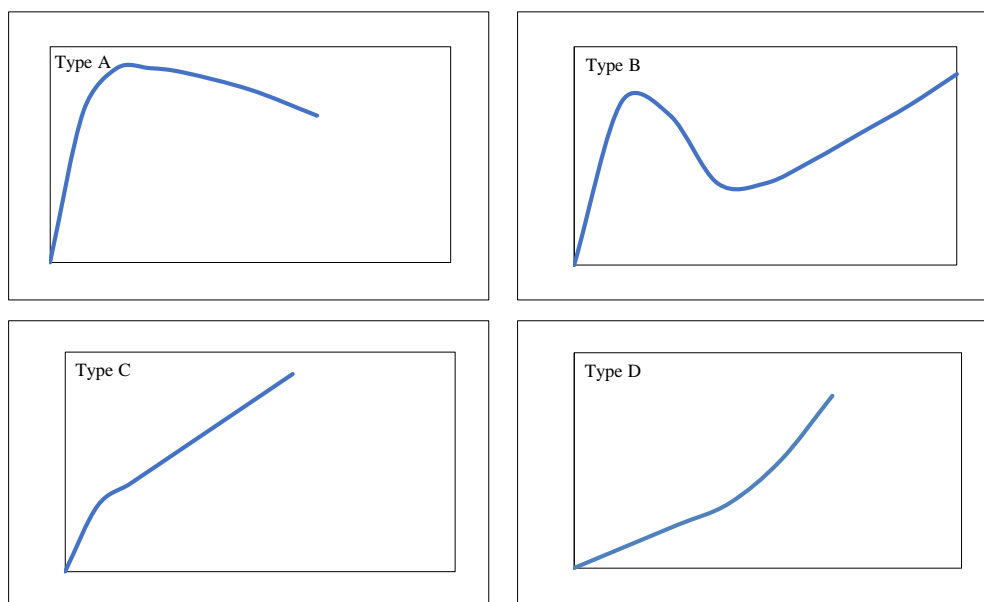


Figure 3. Typical Bond-slip curve for push-out tests on CFST columns

A series of push-out tests with CFST columns with different concrete infills were reported in the literature [3, 5, 7, 11–16]. Prediction models for the bond capacity of circular and square CFST columns were developed using Artificial Neural Networks (ANN) [17]. Thickness of steel tube, compression strength of concrete, and concrete age was fed as input parameters, and using experimental data from the literature, a prediction model was generated that showed better accuracy. To investigate the effects of shrinkage and creep, CFST columns were subjected to a 490-day shrinkage test [18]. Analysis of test results showed that concrete shrinkage and creep had a higher influence on the development of confining effects. It was also observed that the outer tube had no appreciable influence on initial stiffness under service loading conditions. The bond strength of square CFST columns with an H-shaped outer steel casing was also investigated at ambient temperatures [19]. It is reported that chemical adhesion mechanisms predominated at the initial stages of loading. Around 39% of micro-locking mechanisms had a higher influence on the bond capacity of square H-shaped CFST columns.

Investigations on post-fire push-out tests on square and circular CFST were conducted with different temperatures and mass replacement percentages of recycled coarse aggregate (RCA) [20]. It was observed that circular CFST specimens displayed better bond behavior and higher interfacial damage resistance characteristics than square CFST columns. The temperature and RCA had different influences on the test specimens, as the replacement of RCA decreased the bond strength in CFST columns. The bond behavior of CFST with light-weight concrete containing rock-wool waste was investigated under post-fire conditions [21]. The presence of rock wool enhanced the bond strength of CFST columns under post-fire conditions. The provision of internal rings inside steel tubes enhanced the bond strength to an appreciable extent, even at high temperatures [5]. Increasing the axial load ratio also contributes to the development of higher bond strength in CFST columns under post-fire conditions. A series of tests on post-fire push-out tests on elliptical, circular, and square cross-sectional shapes were conducted [22]. Circular CFST columns had higher bond strength among the three shapes, with elliptical CFST columns displaying the lowest bond strength values.

The test results of ambient and post-fire bond strength of CFST columns [21–26] from the literature are shown in Figure 4 for comparison with Japanese, Chinese, and Eurocode values. It can be seen that bond strength in CFST columns has enhanced over the past decade.

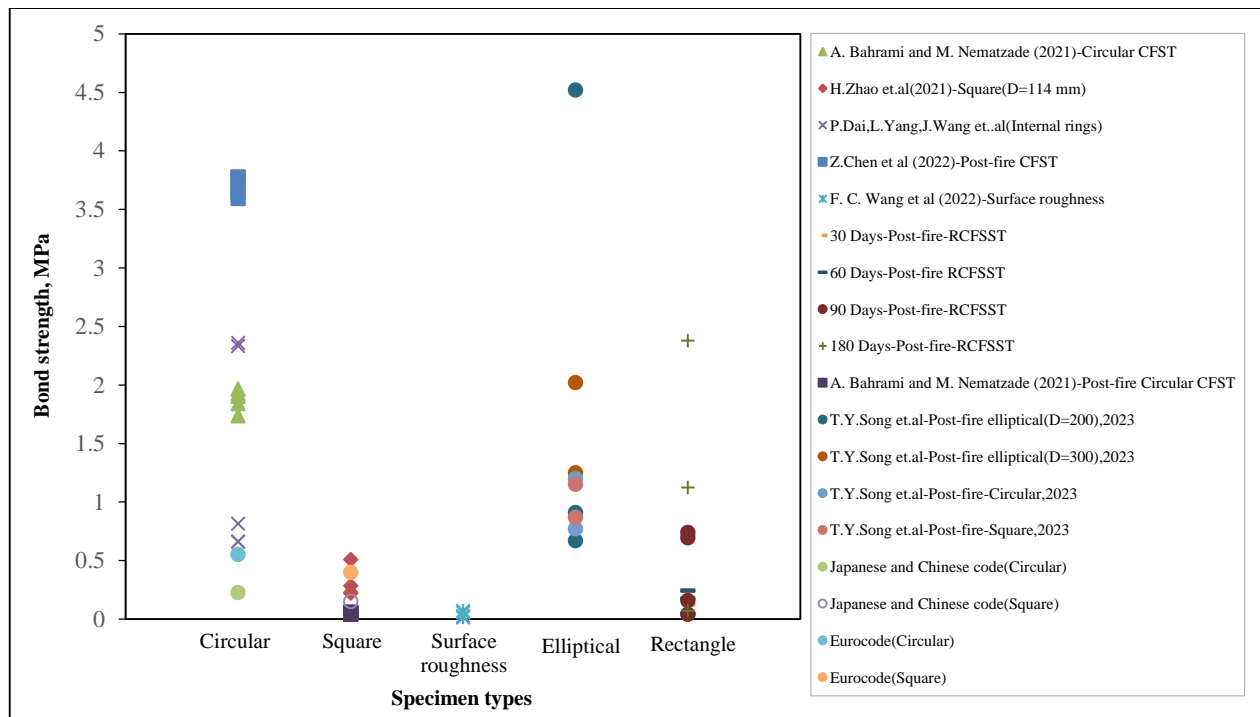


Figure 4. Bond strength of ambient and post-fire CFST columns from test results and literature

The post-fire bond strength of rectangular CFSST columns is little known. Literature studies have always been limited to circular and square CFSST columns. Investigation of other shapes will help the research community gain a better understanding of the behavior of composite columns. Lower bond strengths in rectangular sections make them less demanding. On the other hand, rectangular sections are more feasible during connections, precisely in beam-column connections [4]. They show appreciable resistance to global buckling. Sections other than circular ones would exhibit an uneven temperature distribution [27]. Critical examination of the performance of such sections creates new research interests. This investigation is carried out to provide sufficient research background on the post-fire bond strength of rectangle-shaped CFSST columns.

RCSST columns with varied concrete ages were examined under post-fire conditions in this investigation, and the combined effects of high temperature and concrete age on the bond strength of RCSST columns have been explored. A new set of experimental data on the post-fire bond strength of rectangular concrete-filled stainless steel tubular columns for different concrete ages was recorded for the first time. New τ -s curves were observed from the results. Precise post-fire bond-slip models should be established to perform numerical simulations in the future. The recorded data will assist such research.

2. Experiments

2.1. General

A total of 16 RCSST columns were cast and tested after subjecting the specimens to specific temperature ranges and cooling them to ambient room temperature.

The parameters considered in the test include

- Temperature (T): 600 °C, 800 °C, 1000 °C
- Concrete age: 30 days, 60 days, 90 days, and 180 days

The dimensions of the rectangular columns were 100 mm (depth) \times 50 mm (width) \times 2 mm (thickness). The specimen details are shown in Table 1. The temperature of the specimens was denoted by the letter "T" preceded by the respective numerical, whereas the age of the concrete was denoted by the letter "D" preceded by the numerical denoted in days. For example, in the specimen label "30D600T", "D30" represents the concrete age of 30 days. "600T" represents the temperature of 600 °C. Reference specimens are indicated with the letter "R" followed by their respective concrete ages. For example, in the reference specimen label "R60D", the letter "R" represents the reference specimen, and "60D" represents the concrete age of 60 days.

Table 1. Details of test specimen

S. No.	Specimen ID	Length, L (mm)	Depth, D (mm)	Height, h(mm)	t (mm)	T° C	Nu	τ_u	Su	Curve type
1	R30D	100	50	500	2	20	5.11	0.04	15.28	-
2	30D600T	100	50	500	2	600	16.36	0.127	17.69	1
3	30D800T	100	50	500	2	800	93	0.727	26.29	3
4	30D1000T	100	50	500	2	1000	-	-	-	-
5	R60D	100	50	500	2	20	8.13	0.05	24.92	2
6	60D600T	100	50	500	2	600	90.41	0.244	35.79	5
7	60D800T	100	50	500	2	800	-	-	-	-
8	60D1000T	100	50	500	2	1000	64.56	0.175	28.91	5
9	R90D	100	50	500	2	20	7.43	0.04	37.90	2
10	90D600T	100	50	500	2	600	20.88	0.158	3.01	1
11	90D800T	100	50	500	2	800	94.93	0.742	35.70	1
12	90D1000T	100	50	500	2	1000	88.83	0.695	35.52	4
13	R180D	100	50	500	2	20	37.77	0.275	20.75	5
14	180D600T	100	50	500	2	600	-	-	-	-
15	180D800T	100	50	500	2	800	143.9	1.125	25.21	1
16	180D1000T	100	50	500	2	1000	306.07	2.394	22.06	4

2.2. Material Properties

2.2.1. Stainless Steel

Tensile tests were carried out to determine the material properties of stainless steel using tensile coupons cut from the specimens. The test was conducted using an INSTRON tensile testing machine in accordance with ASTM E8. In order to measure the longitudinal strains, strain gauges were positioned along the longitudinal region of the coupons, and readings were recorded using data acquisition systems. An extensometer is fixed to the coupon up to the elastic limit to determine the modulus of elasticity of the material. The material properties obtained from the test are tabulated in Table 2, where E_0 is the elastic modulus, $\sigma_{0.2}$ is 0.2% proof strength, σ_u is the ultimate stress, and μ_s is the Poisson ratio of the material.

Table 2. Properties of stainless-steel

Section	$\sigma_{0.2}$ (MPa)	σ_u (MPa)	E_0 (MPa)	μ_s
SS304	346	715	190,000	0.3

2.2.2. Concrete

Concrete of grade M40 was filled inside the rectangular hollow stainless-steel tubes. Standard concrete cubes of nominal dimension (150 mm \times 150 mm \times 150 mm) were cast along the test specimens and tested for their compressive strength. The measured average compressive strength of concrete is listed in Table 3. At high temperatures, concrete with a higher paste-aggregate ratio had a severe strength reduction compared to normal-strength concrete (NSC) mixes. Hence, for the experiments involving high temperature exposure, a moderate grade of M40 was adopted.

Table 3. Compressive strength of concrete cube specimens

Specimen	Compressive cube strength, f_c' (MPa)	Mean value
C600	50.75	51.55
	49.46	
	54.44	
C800	55.95	54.42
	52.88	
	54.44	
C1000	55.24	55.27
	55.11	
	55.46	

2.3. Selection of Parameters

The temperature range of 600 to 1000 °C was chosen as the desired target temperature for this investigation. The reduction rate of concrete's compressive strength increases between 400–800 °C [28, 29]. In the case of steel, stainless steel exhibits higher mechanical strength due to the effect of cold working [30]. However, after 700 °C, the effect of cold working becomes less influential as stainless steel attains recrystallization temperature [31]. Since a critical point is attained for both concrete and stainless steel between 400–800 °C, it is essential to investigate the adequacy of bond-strength in these temperature ranges. Another parameter investigated in this study is the age of concrete. As the age of concrete increases, shrinkage effects take place. After 180 days of curing, the influence of the steel type (carbon or stainless steel) on the bond strength of CFST columns is minimized. Hence, CFST specimens were cured for 28 days, 60 days, 90 days, and 180 days in this experiment to examine the effects of high temperatures on different concrete ages. Establishing the bond stress-slip relationship for CFST columns with older concrete assists in numerical simulations. The sensitivity of other values of the selected parameters is beyond the scope of this experiment and will be addressed through numerical simulations in the future.

2.4. Preparation of the Test Specimens

Rectangular tubular columns of SS304 stainless-steel material were bought from the vendor and cut into desired lengths of 500 mm for the tests. Stainless-steel tubes had 2B surface finishes and were in polished condition. The chemical composition of the stainless steel adopted in the tests is tabulated in Table 4. Hollow tubes were then filled with concrete. As this study was carried out by a push-out testing procedure, the top and bottom parts of the stainless steel were filled with foam material up to 15 mm, such that the concrete was filled up to a certain limit inside the hollow tube, leaving a gap of 15 mm on either side of the hollow tube. After casting, the specimens were cured inside a curing tank for 30 days, 60 days, 90 days, and 180 days, respectively. Casting and curing conditions were maintained evenly to ensure homogeneous conditions. After curing, both ends of the rectangular CFSST columns were closed with mild steel plates to prevent direct exposure of fire to concrete and placed inside an electric furnace. The electric furnace has the capability of supplying a maximum temperature of 1000 °C.

Table 4. Chemical composition of Austenitic stainless steel (SS304)

ASTM Designation	% by Mass				
	Carbon (C)	Silica (Si)	Manganese (Mn)	Chromium (Cr)	Nickel (N)
314	0.20	1.5-2.5	2.00	24.00-26.00	19.00-22.00

2.5. Fire Test Procedure

In order to expose the test specimens to high temperatures, 12 specimens, excluding the reference specimens, were placed inside an electric furnace, as shown in Figure 5. A heating rate of 10 °C/min was maintained. The adopted heating rate was kept constant for all the test specimens. The temperature-time curve adopted in this study consists of four parts: first, the specimens were heated to the desired temperature range (600, 800, or 1000 °C) and next, the temperature was maintained for a desired duration to ensure uniform temperature distribution across the specimen; furthermore, the specimens were subjected to cooling without the influence of an external environment; and lastly, the specimens were allowed to cool down to room temperature inside the furnace. It is to be noted that the air-cooled specimens had fewer effects on post-fire strength deterioration, and hence the specimens were naturally allowed to cool to ambient temperatures. After reaching a target temperature of 30 °C, the specimens were taken out of the furnace. A sudden drop in temperature can be observed from the temperature-time curve, as shown in Figure 6. The electric furnace took about 10–13 hours to reach ambient temperature. The temperature-time curve was observed to be uniform for all the specimens.



Figure 5. Electrical furnace for post-fire tests

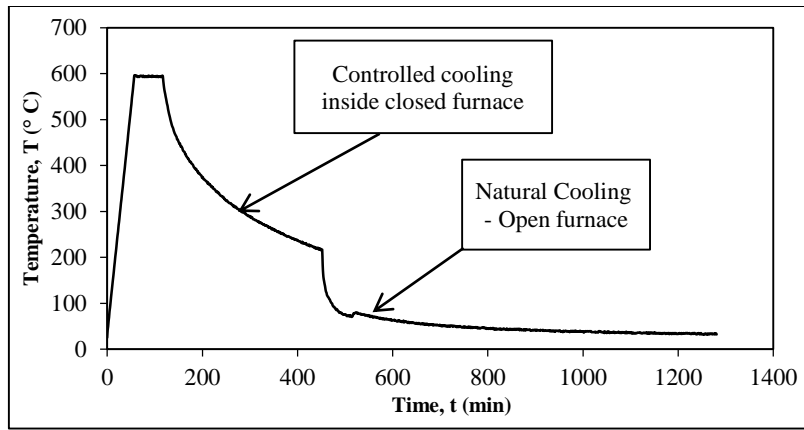


Figure 6. Heating and cooling curve adopted in the study

2.6. Loading Procedure

A detailed flowchart of the methodology adopted in this study is shown in Figure 7. In order to find the bond strength of RCFSST columns, the concrete inside the steel tube has to be pushed out, and the load required to push out or cause slippage of the concrete from the hollow tube was taken as the bond strength of the specimen. Hence, after cooling the specimens to room temperature, the specimens were then loaded on the Universal Testing Machine (UTM) at the Strength of Materials Laboratory, Vellore Institute of Technology, Vellore, India. A steel block of size (95 mm x 45 mm x 50 mm) was placed over the top layer of the specimens such that the steel block bears the applied load and transfers it to the concrete present inside the hollow tube.

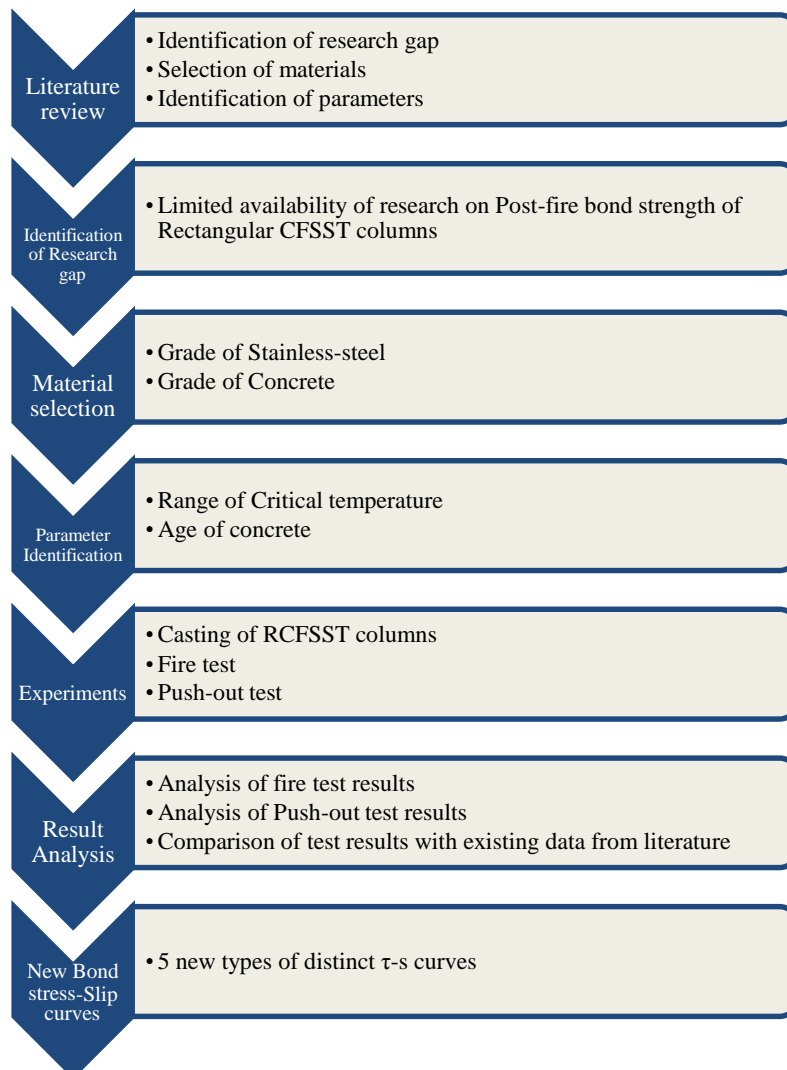


Figure 7. Flow chart for methodology adopted in the study

When a load was applied using UTM, the steel block placed above the concrete layer pushed the concrete down, causing slippage of the concrete. The loading setup is shown in Figure 8. An LVDT was placed at the bottom of the specimen to measure the displacement of the concrete from the outer steel tube. Axial displacements were also observed by recording the movement of the cross-head travel of the UTM. The maximum load obtained during the test is considered the load required to cause slippage, and bond stress is calculated using the obtained load from the experiments. The experiment was carried out without any discrepancies.

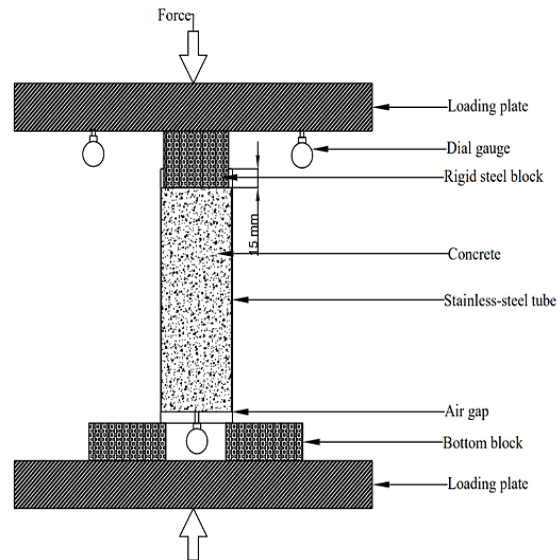


Figure 8. Push-out test setup for post-fire RCFSSST columns

3. Test Results and Discussion

3.1. Fire Test Results

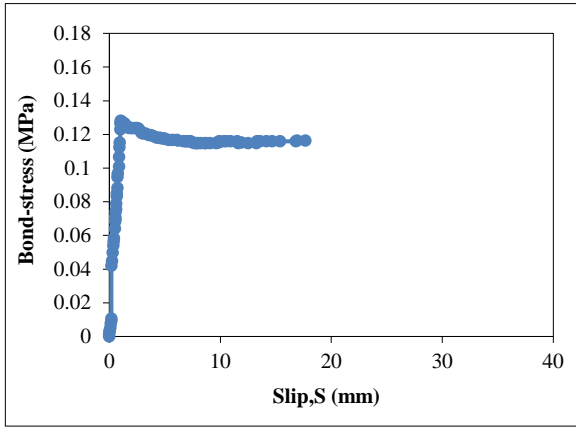
Generally, stainless steel exhibits a silvery-white color. When the specimens were taken out of the furnace after attaining an ambient temperature, appreciable color changes were noted on the outer surface of the stainless-steel material, as shown in Figure 9. The color of the outer tube gradually became darker, from silvery white at room temperature to grayish black at 1000 °C. Small flakes of the stainless-steel material were ruptured from the surface of the steel tube at 1000 °C. Higher integrity of the concrete was observed at lower temperatures and prevailed to a certain extent during the loading conditions. Around 800 °C, minute cracks were observed on the concrete surface, and minute parts of the concrete disintegrated at 1000 °C.



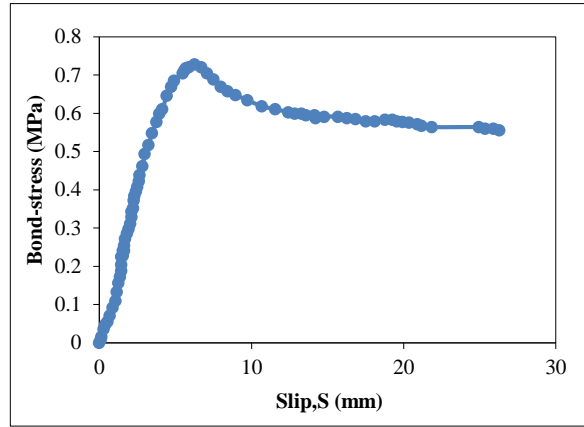
Figure 9. Post-fire test on RCFSSST columns

3.2. Push-out Test Results

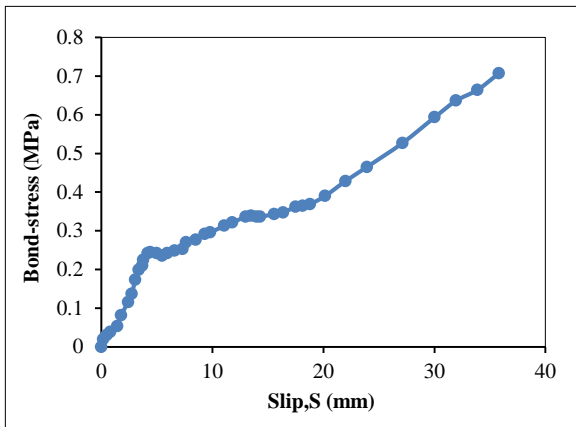
Figure 10 shows the bond(τ)-slip(s) curves of the test specimens. The following characteristics were observed from the bond stress-slip curve:



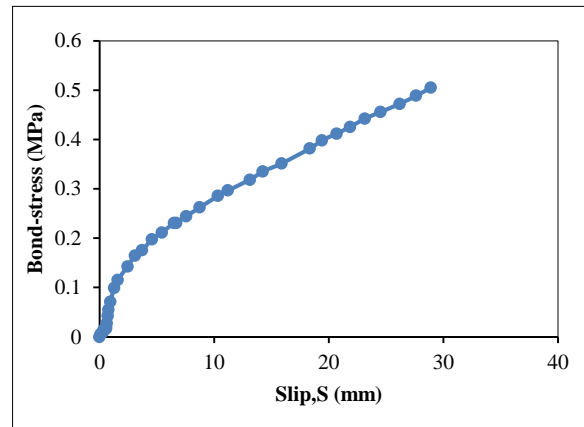
i) τ -s curve of specimen 30D600T



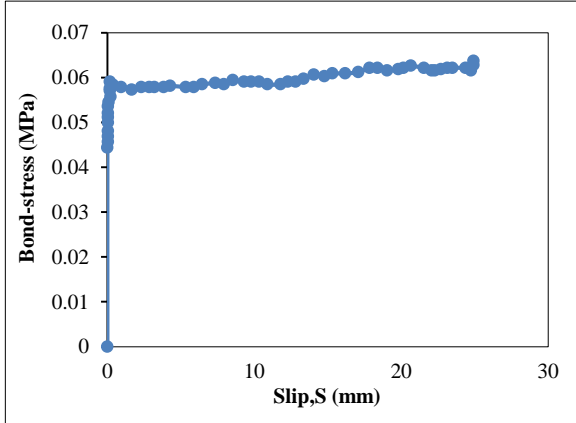
ii) τ -s curve of specimen 30D800T



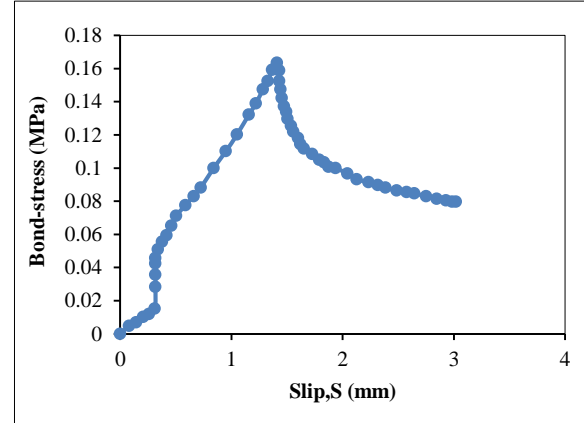
iii) τ -s curve of specimen 60D600T



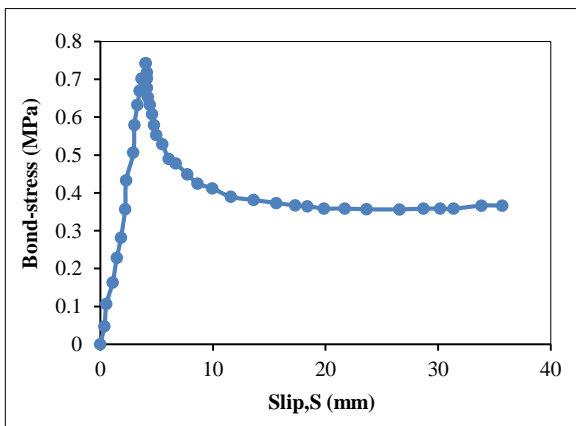
iv) τ -s curve of specimen 60D1000T



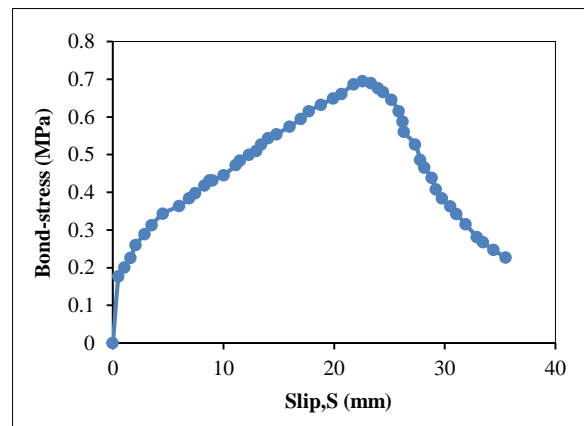
v) τ -s curve of specimen R60D



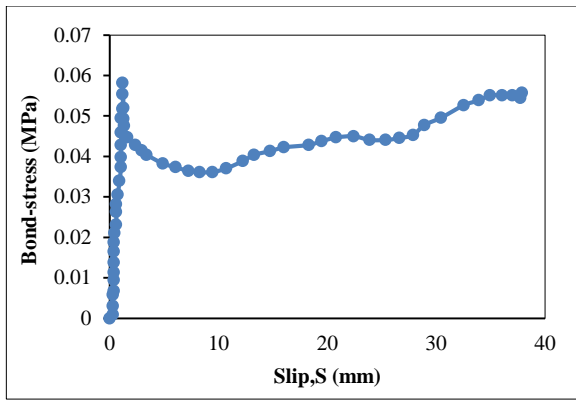
vi) τ -s curve of specimen 30D600T



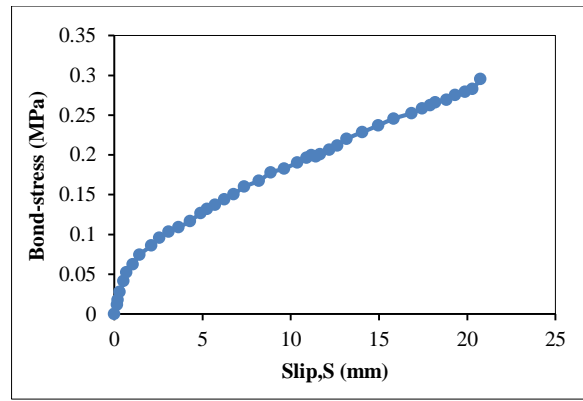
vii) τ -s curve of specimen 90D800T



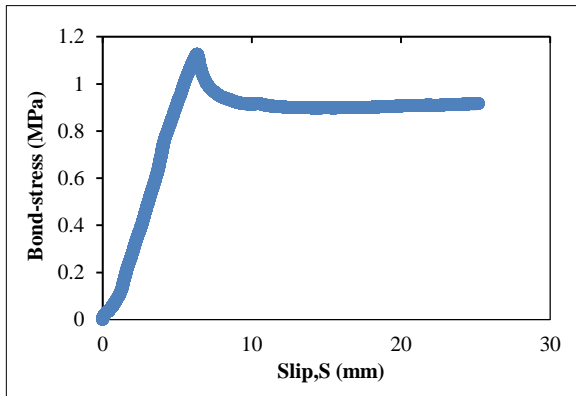
viii) τ -s curve of specimen 90D1000T



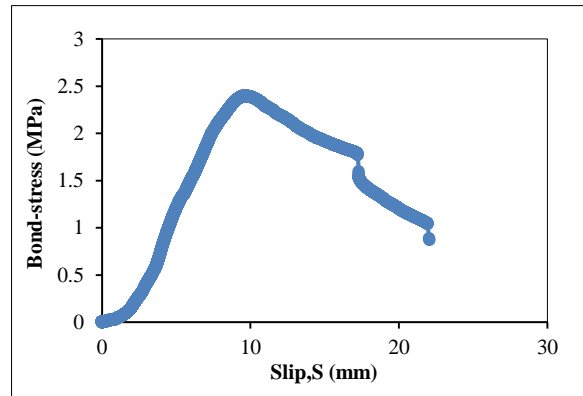
vix) τ -s curve of specimen R90D



x) τ -s curve of specimen 180D600T



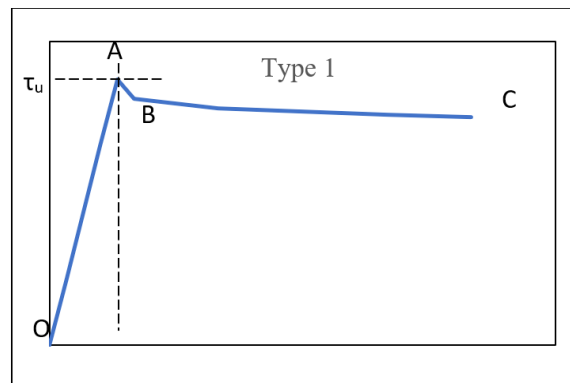
xi) τ -s curve of specimen 180D800T



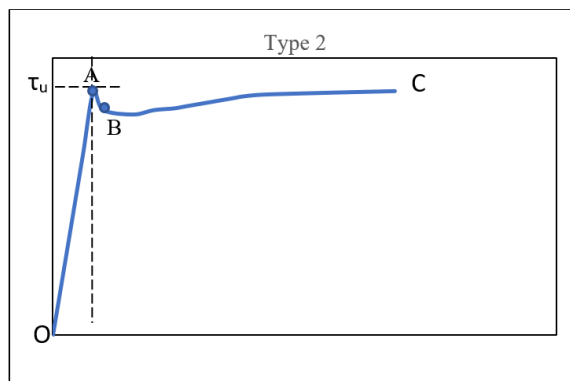
xii) τ -s curve of specimen 180D1000T

Figure 10. Bond-stress(τ)-Slip(s) curves obtained from push-out test of RCFSST specimens

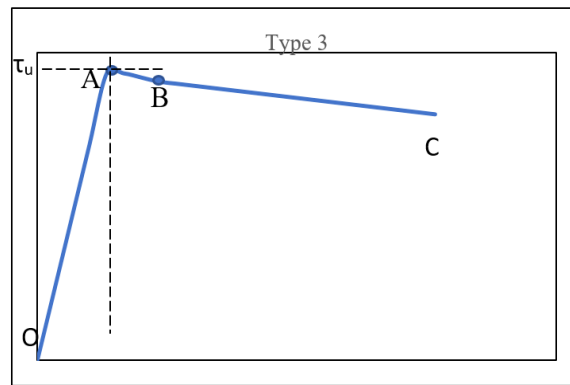
- The bond stress-slip curves can be categorized into five different types of curves, namely Type 1, Type 2, Type 3, Type 4, and Type 5, respectively, as shown in Figure 11. However, the effect of temperature and concrete age was found to be random.



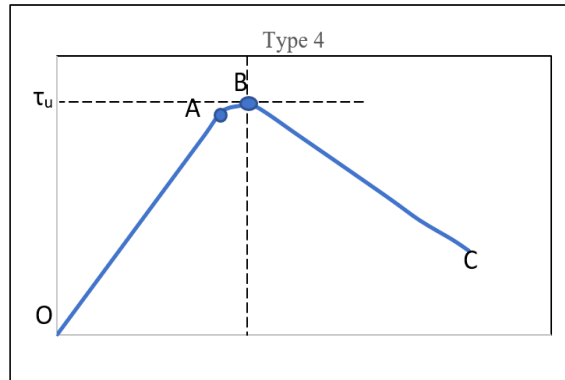
i) Type 1 τ -s curve



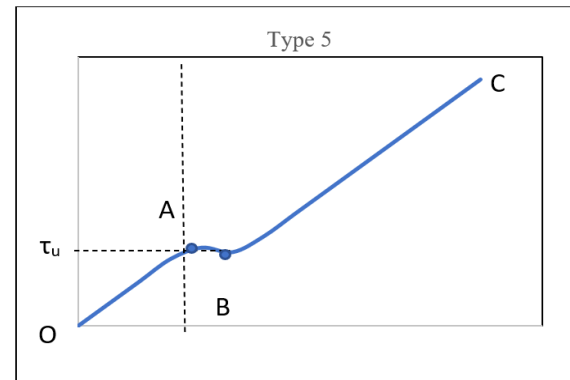
ii) Type 2 τ -s curve



iii) Type 3 τ-s curve



iv) Type 4 τ-s curve



v) Type 5 τ-s curve

Figure 11. Classification of τ-s curves obtained from the test results

- The Type 1 curve had three stages: i) the initial linear stage (OA), where the bond stress gradually increases linearly; ii) the non-linear stage (AB), where the bond stress drops with a gradual slope; and iii) the linear stage (BC), where the bond stress has a further decrease. The Type 2 curve also displayed three stages: i) the initial linear stage (OA), where the bond stress had a linear increase; and ii) & iii) two non-linear stages, Curves AB and BC. Unlike the Type 1 curve, the bond stress had a gradual increase in the later stage (BC);
- The Type 3 curve is also similar to the Type 1 and Type 2 curves. The only difference is that the Type 3 curve exhibited a gradual slope (BC) after achieving the non-linear stage (AB), whereas in the Type 1 and Type 2 curves, a steep slope was observed in later stages. The Type 4 curve is a two-stage curve with an initial linear stage (OA) and a non-linear stage (AB). The Type 5 curve displayed a similar trend as the Type 2 curve, but at the third stage (BC), the rate of increase in bond stress was so high;
- Based on the occurrence of the curve shapes observed from the test results, four specimens (33%), namely 30D600T, 90D600T, 90D800T, and 180D800T, exhibited Type 1, three specimens, namely 60D600T, 60D1000T, and R180D, presented a Type 5 curve (25%), two specimens, R90D and R60D, showed a Type 2 curve (16%), and two specimens, 90D1000T and 180D1000T, displayed a Type 4 curve (16%). The specimen labeled 30D800T exhibited a Type 3 curve (8.3%);
- The bond strength of the specimens can be determined from the bond stress-slip curve obtained from the test results. For specimens presented on the on the Type 1, Type 3, and Type 4 curves, the maximum point on the τ-s curve was

taken as the ultimate bond strength (τ_u) of the specimens. For specimens that exhibited Type 2 and Type 5 curves, prediction of ultimate bond strength becomes challenging since the τ -s curve kept increasing through the test, and hence no definite point can be taken as τ_u . However, a change of slope at BC was noted in Type 2 and Type 5 curves. The ascending stage BC of both the Type 2 and Type 5 curves had a lower slope than the initial linear stage (OA), and hence point A is taken as τ_u in both cases.

3.3. Influence of parameters on bond strength of RCFSSST columns

3.3.1. High Temperature

The influence of high temperatures on the bond strength of RCFSSST column specimens with different concrete ages is shown in Figure 12. From the test results, it is noted that at initial ages of concrete, the impact of increasing the temperature was much higher. The bond strength of the test specimens showed a substantial increase up to 800 °C for all concrete ages considered in this study. The bond strength test specimens can be categorized into two distinct types based on their test results: i) Type A – Specimens with a concrete age of 30 days, 60 days, and 90 days; and ii) Type B – Specimens with a concrete age of 180 days.

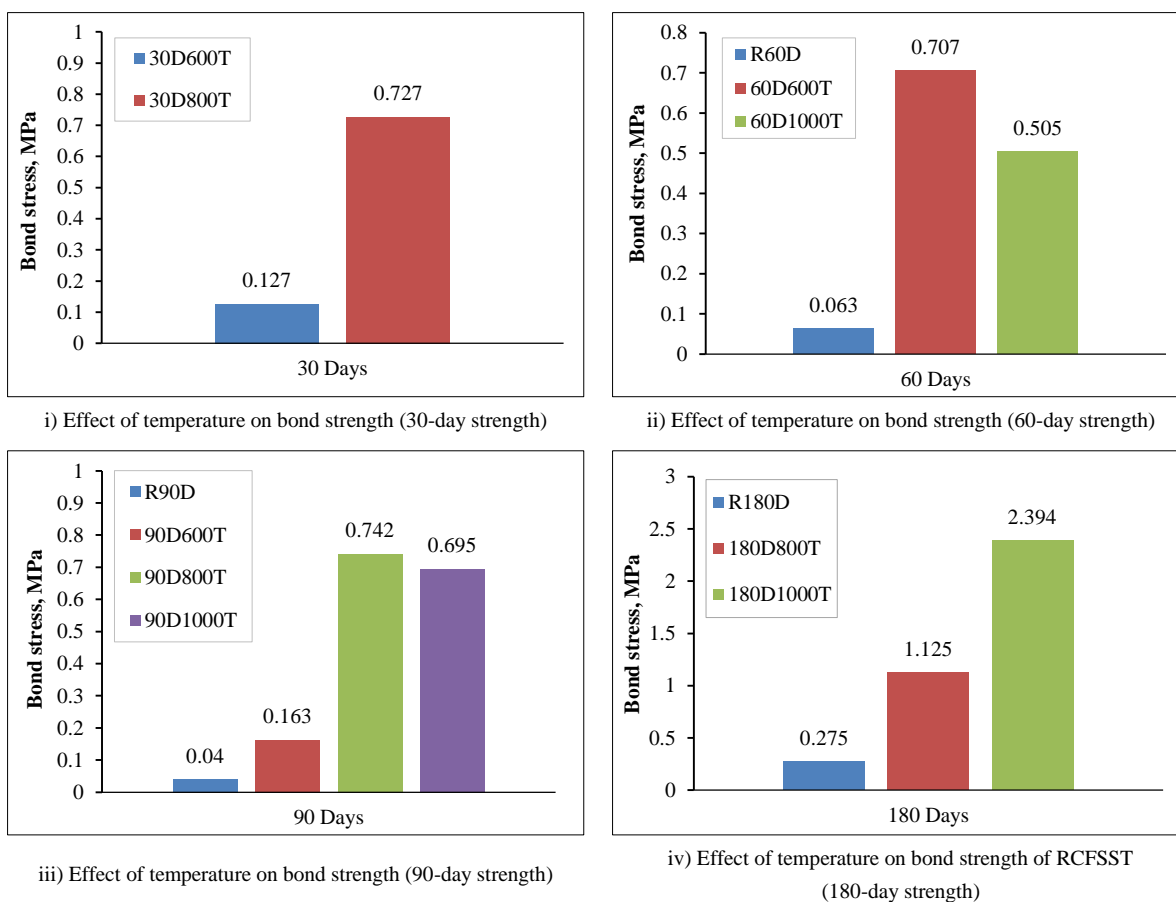


Figure 12. Effect of high temperature on bond-strength of RCFSSST columns for various concrete ages

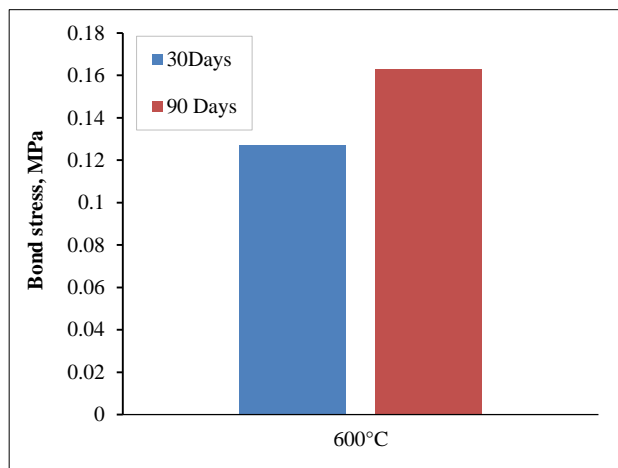
Type A – Specimens in this category exhibited an increase in bond strength up to 800 °C. The influence of temperature was higher for the initial age of concrete. In other words, the rate of increase in bond strength of the test specimens was influenced by concrete age, as the rate deteriorates when concrete ages more. However, beyond 800 °C, the increase in temperature had a detrimental effect on the post-fire bond strength of RCFSSST columns. In comparison with reference specimens that were tested without any fire exposure, a significant increase in bond strength was observed when the temperature was raised to 600 °C, as shown in Figures 12(i)–12(iv). The % increase in bond strength was much higher when the temperature was increased to 600 °C than the % increase in bond strength when the temperature was elevated from 600 °C to 800 °C. All the specimens in Type A displayed a similar trend. The rate of decrease in bond strength beyond 800 °C was also influenced by concrete age, as the rate was reduced with an increase in concrete age. In other words, the rate of decrease in bond strength had an inversely proportional relationship with concrete age.

Type B – Specimens in this category displayed a significant increase in bond strength for all temperature ranges. The influence of temperature was much higher for specimens of this type than for Type A specimens. Unlike Type A specimens, which had a decrease in bond strength beyond 800 °C, Type B specimens exhibited superior bond strength

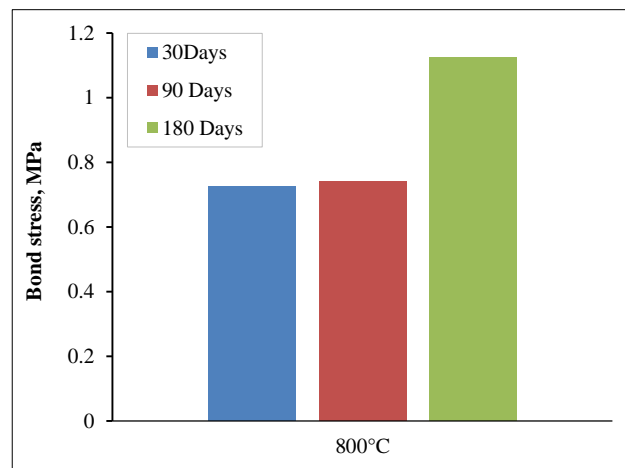
when the temperature was increased to 1000 °C. However, the rate of increase in bond strength decreases with an increase in temperature. Below 800 °C, the rate of increase in bond strength was much higher than the increase rate from 800 °C to 1000 °C. The rate of increase in bond strength of Type B specimens displayed a higher percentage than the rate of increase in bond strength of Type A specimens within identical temperature ranges. Type B specimens displayed much higher bond strengths than type A specimens. The maximum bond strength observed in Type A specimens was 0.727 MPa, whereas in Type B specimens, the maximum bond strength was 2.394 MPa. Type B specimens presented τ -s curves of Type 1, Type 4, and Type 5, whereas Type A specimens demonstrated all five curve types.

3.3.2. Concrete Age

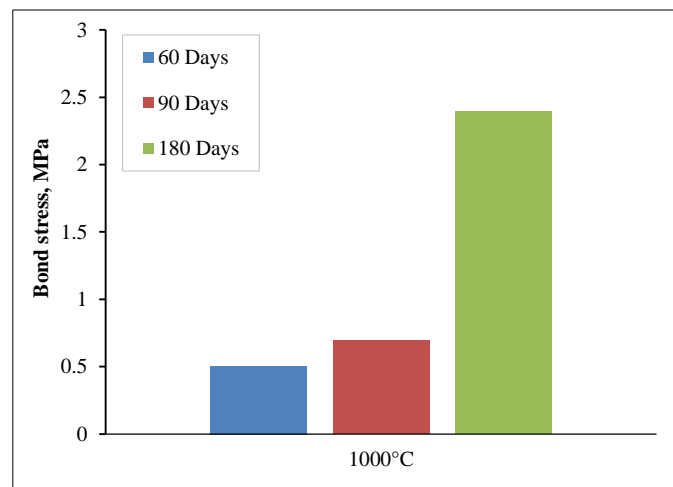
Specimens under the same temperature range for different concrete ages were compared to investigate the influence of concrete age on the post-fire bond strength of RCFSSST columns, as shown in Figure 13. It was very clear that the increase in concrete age maximizes the bond strength of post-fire RCFSSST columns. At 600°C, the specimens with a 90-day concrete age demonstrated an increase in bond strength when compared to specimens with a concrete age of 30 days. However, at 800 °C, the increase in bond strength was not much appreciable for specimens with concrete ages of 30 days, 60 days, and 90 days. At 1000 °C, the influence of concrete age was much higher. The post-fire bond strength of RCFSSST column specimens exhibited a higher rate of increase as the concrete became older. At all three temperatures considered in this study, an increase in concrete age resulted in an increase in the post-fire bond strength of the RCFSSST column specimens. A higher rate of increase in bond strength was observed for specimens with a concrete age of 180 days. Specimens with a concrete age of 180 days exhibited better performance under all the temperature ranges adopted in this study. The maximum post-fire bond strength achieved by the specimen 180D1000T, which was cured for 180 days and exposed to a temperature of 1000 °C. Comparing the influence of temperature and concrete age parameters, concrete age provided a significant contribution to maximizing the post-fire bond strength of RCFSSST columns.



i) Effect of concrete age on bond strength (600°C)



ii) Effect of concrete age on bond strength (800°C)



iii) Effect of concrete age on bond strength (1000°C)

Figure 13. Effect of concrete age on post-fire bond strength of RCFSSST columns

4. Bond Strength of Concrete Filled Stainless-Steel Tubular Columns

4.1. Bond Strength at Ambient Temperature

Analyzing the τ -s curves of RCFSSST columns at ambient temperatures, the 60-day specimen and the 90-day specimen exhibited Type-2 curves, which had a three-stage τ -s curve, namely one linear and two non-linear curves, as mentioned in the previous sections. The slope of the curve OA decreases with an increase in concrete age. The test specimen R60D displayed a steeper slope than the specimen R90D, as shown in Figure 14. Generally, the linear region (OA) is associated with chemical adhesion and micro-locking mechanisms. As concrete ages, the adhesive mechanism and micro-locking mechanism degrade, causing the resulting curve. Comparing the point of inflection B of the τ -s curves of ambient temperature test specimens, specimens with higher concrete age had a sharp inflection point B. From the test results, it was very clear that the specimen with a 90-day concrete age displayed higher non-linearity in the later stage (BC) of the τ -s curve. Macro-locking attributes to the “BC” region of the curve. As the concrete ages, shrinkage increases, resulting in a reduced macro-locking mechanism.

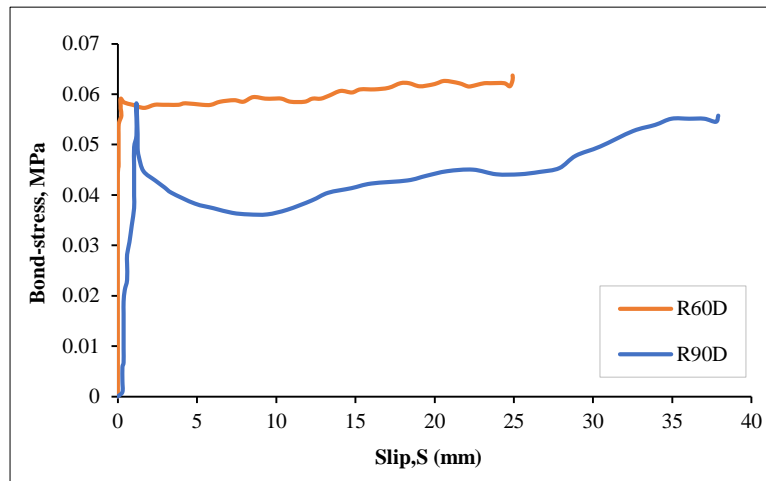


Figure 14. τ -s curve for ambient temperature RCFSSST columns with different concrete ages

Meanwhile, the specimens displayed a very minor change in τ_u , for different concrete ages. The reduction factors obtained from the test results for ambient-temperature RCFSSST specimens and the reduction factors reported in the literature [21, 23, 32, 33] for various parameters are shown in Figure 15. It was clear from Figure 15 that the bond strength can be enhanced by providing internal rings, but on the other hand, the change in surface roughness of the internal steel tube also contributed to a greater extent. An increase in CRA content also contributed to enhancing bond strength. Light-weight concrete-filled steel tubes incorporating rook wool waste had a declining strength compared to normal CFST specimens.

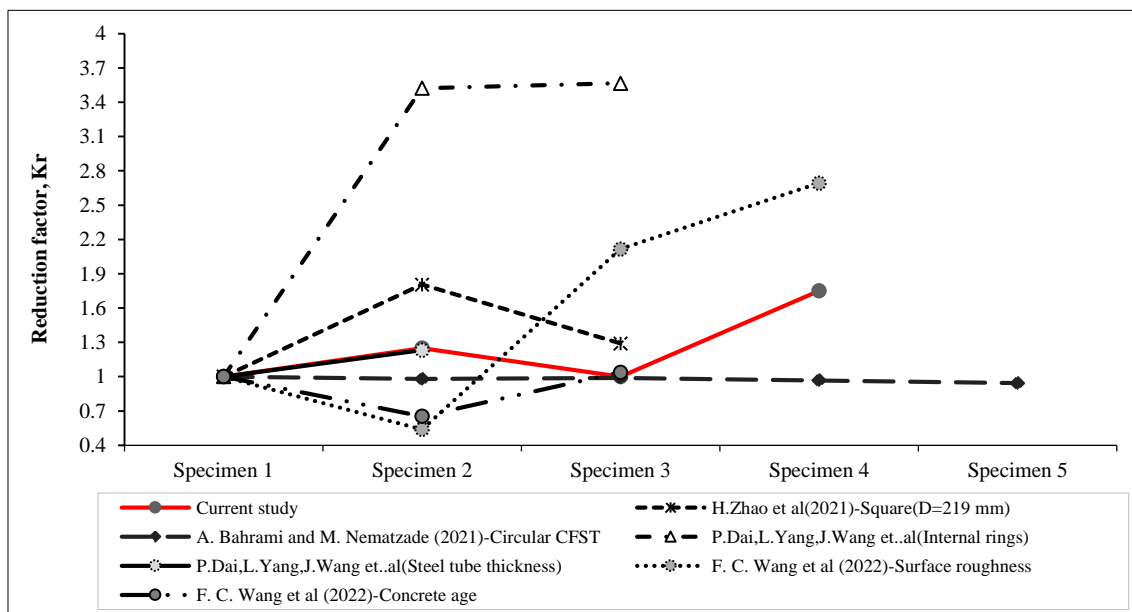


Figure 15. Reduction factors of ambient temperature bond strength of CFST columns from test results and literature

4.2. Bond Strength of CFSST and CFST Columns Under Post-Fire Condition

The characteristics of the τ -s curve of RCFSST specimens were examined in each temperature range, as shown in Figures 16-a to 16-c. Around 600°C, the RCFSST specimens displayed Type 1 and Type 5 τ -s curve characteristics. Type 1 curve was associated with 30 and 90-day specimens, while 60-day specimens displayed type 5 curve features at 600 °C. The linear region OA of the τ -s curve for 30 and 90-day specimens demonstrated similar slopes, whereas higher slope values were noted in 60-day specimens. The τ -s curve of 30 days and 90 days displayed a variation after the inflection point B of the τ -s curve, whereas both specimens exhibited a declining trend in their later stages (BC). In the case of the 60-day specimen, the curve BC had a positive slope.

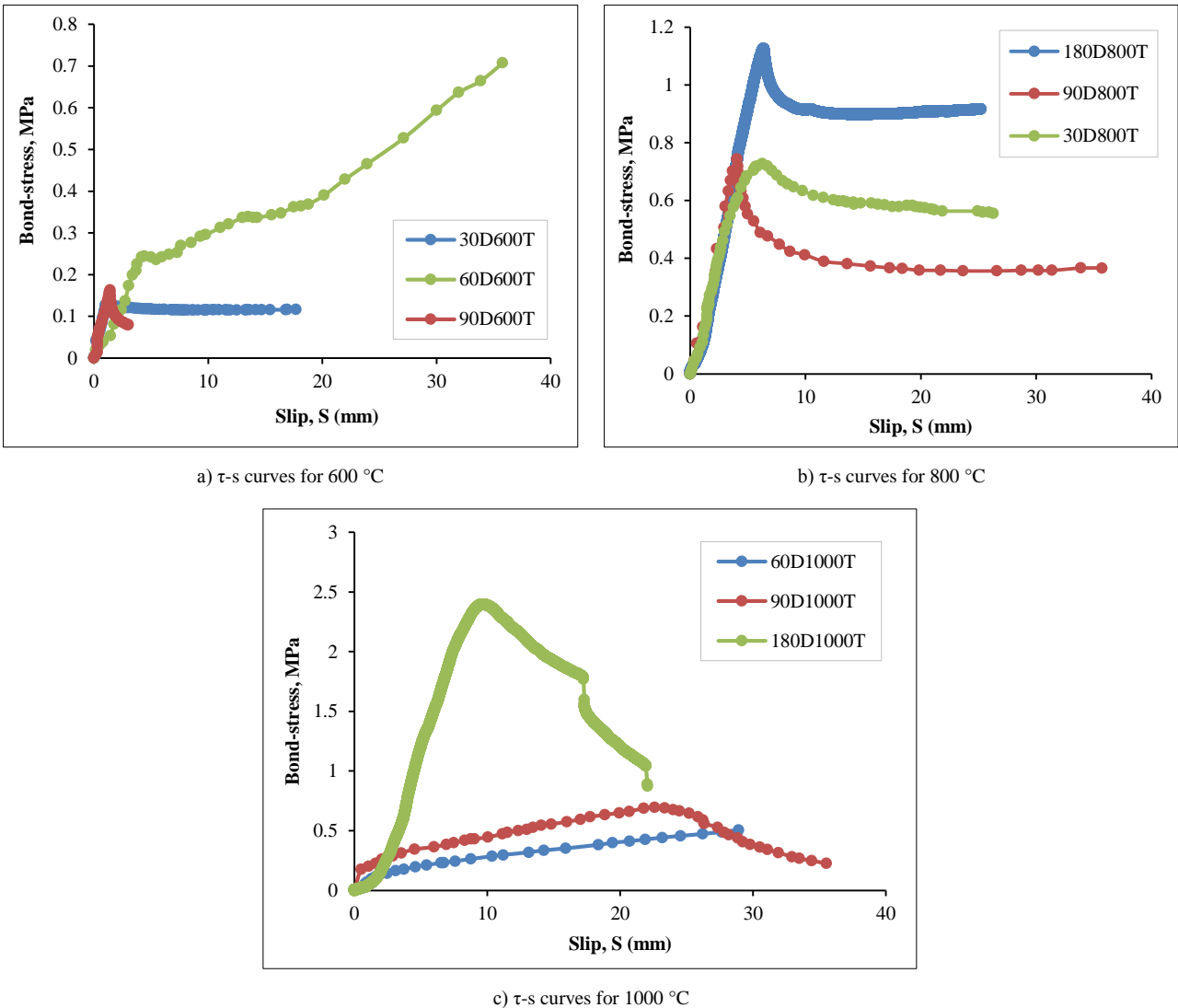


Figure 16. Comparison of τ -s curves for different temperature ranges

At 800 °C, the slope of the linear curve OA for all the specimens, irrespective of their concrete age, displayed similar trends. Except for the 30-day specimen, all the other specimens had a Type 1 classification with three-stage curve characteristics. At 1000 °C, the linear region OA of the τ -s curve for the specimens with lower concrete ages (Type A) was short in comparison with specimens with a concrete age of 180 days (Type B). It is evident that at 180 days, chemical adhesion and micro-locking were ineffective, resulting in shorter linear branch OA. The linear region OA was followed by a short AB region, which indicates the loss of bond was sudden. The specimens exhibited a larger BC region of the τ -s curve than Type A specimens. Comparisons of bond strength for different concrete ages are shown in Figures 17 (a) to (d). As bond strength in rectangular columns is mostly governed by the macro-locking mechanism, an increase in the non-linear portion BC verifies the intactness of macro-locking. Type B specimens at this temperature zone were associated with the Type 4 category of the τ -s curve. The post-fire bond-strength reduction factor (k_r) obtained from the test results was compared with the reduction factors (k_r) reported in the literature [20–22], as shown in Figure 18.

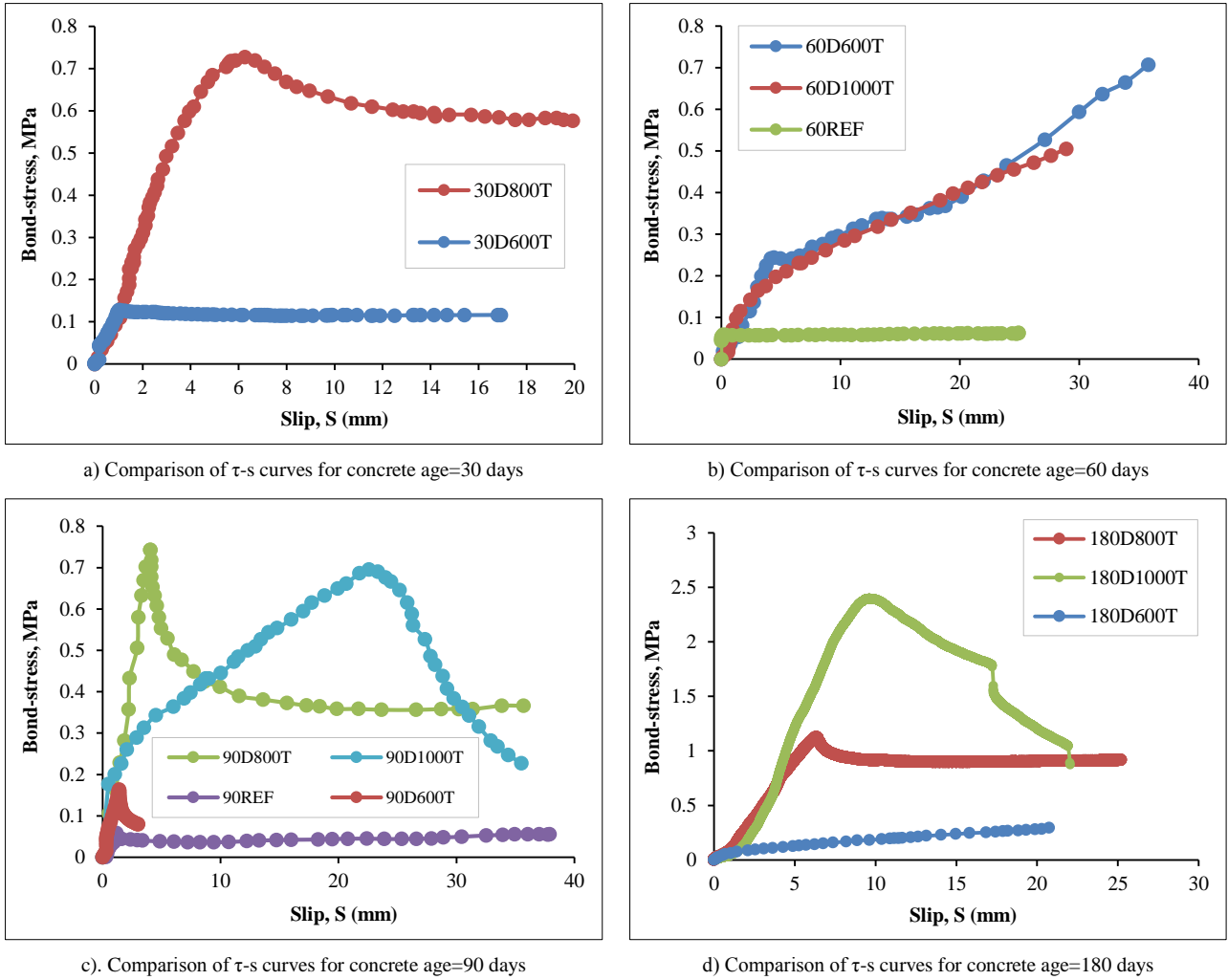


Figure 17. Comparison of τ -s curves for different concrete ages

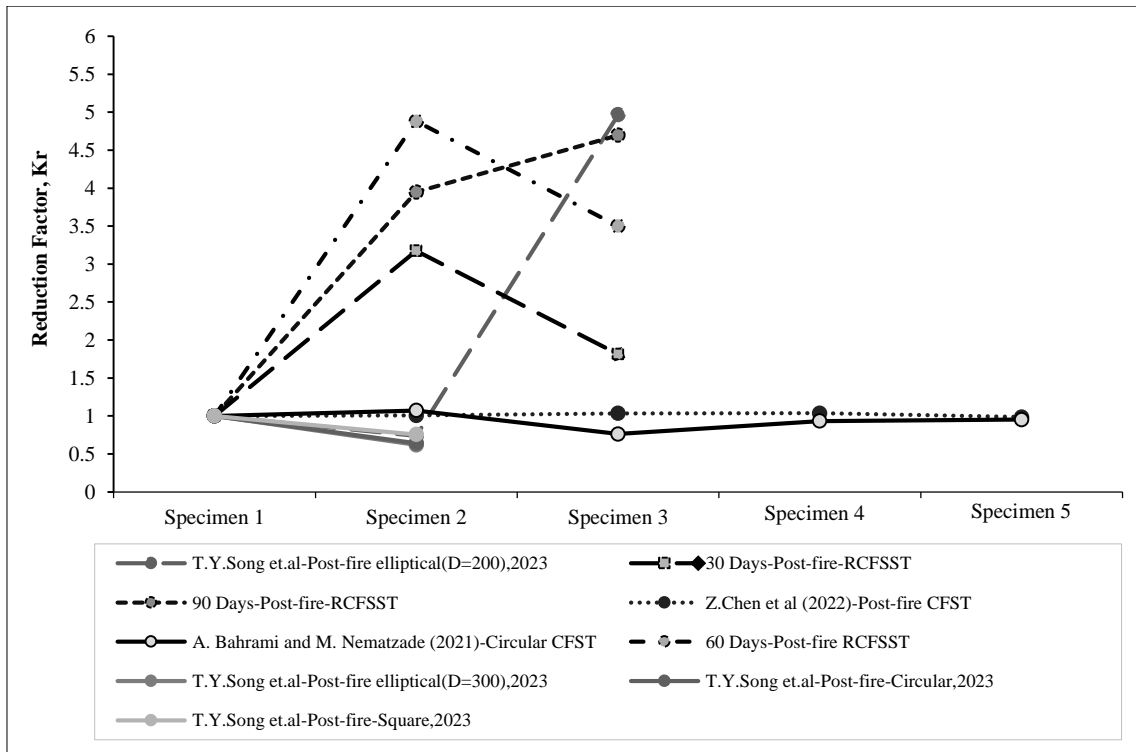


Figure 18. Comparison of reduction factors of post-fire bond strength of CFST columns from test results and literature

4.3. Comparison of Experimental Data with Existing Literature

A comparison of the relative increase in bond strength of CFST columns is shown in Figure 19. At ambient temperatures, rectangular CFSST columns displayed lower bond strength in comparison with other shapes of CFST columns [22]. Circular CFST columns exhibited higher bond strength, followed by square and rectangular specimens, with elliptical CFST having the least bond strength at earlier ages of concrete. It is obvious that hoop stress developed in circular CFST columns enhances bond capacity [5]. But as the age of concrete increased, the relative increase in bond strength of rectangular CFSST columns had substantial growth. In other words, the rate of increase in bond strength from the 30-day curing period to 180 days was noted to be significantly higher in rectangular CFSST columns. Around a 68% increase in bond strength was observed in rectangular CFSST columns with 180-day curing. In the case of circular columns, no appreciable increase in bond capacity was observed, as reported in the literature [22].

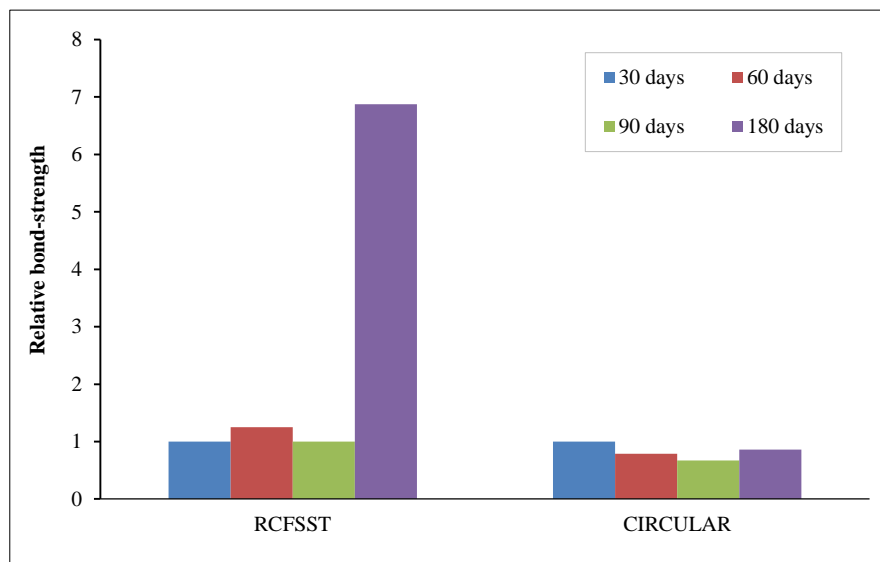


Figure 19. Comparison of relative bond-strength for different concrete ages from the literature [22] at room temperature

A comparison of the relative increase in bond strength for different shapes of CFST columns at 600 °C and ambient temperatures, as reported in the literature, is shown in Figure 20. At earlier concrete ages, around 600 °C, the post-fire bond strength of square-shaped specimens exhibited an appreciable increase in bond capacity in comparison with ambient-temperature square specimens. The rate of increase was highest in square specimens, followed by circular and rectangular specimens. However, higher bond strength capacity was displayed by circular CFST columns. A comparison of different shapes and their relative increase in bond strength in comparison with room-temperature specimens is shown in Figure 21.

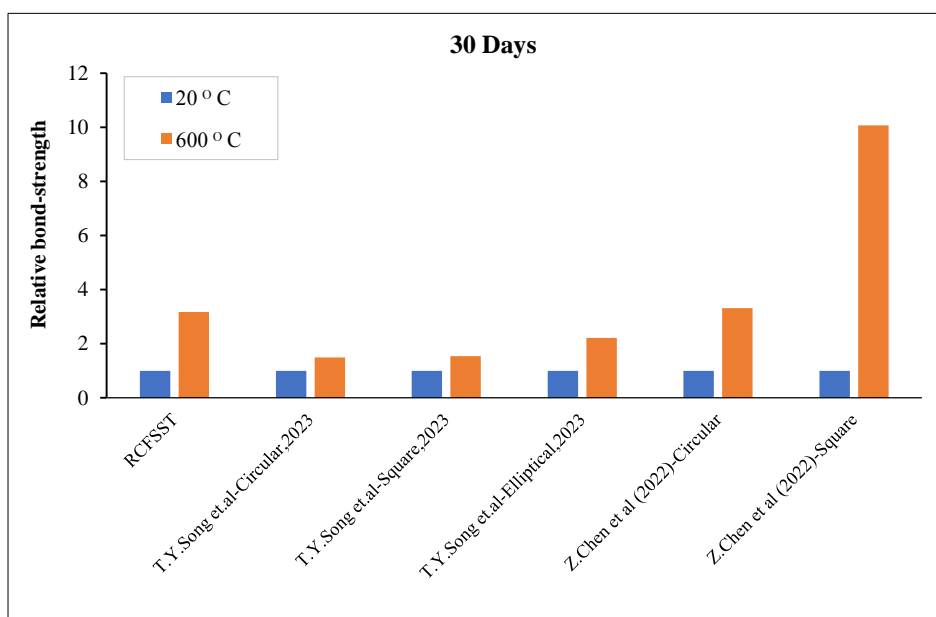


Figure 20. Comparison of post-fire bond-strength for different shapes of CFST from the literature [20, 22]

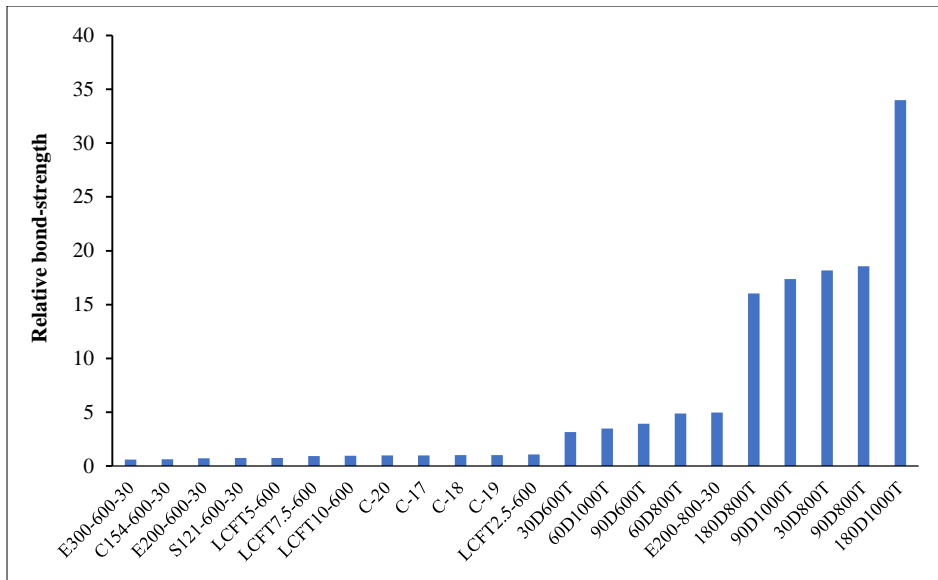


Figure 21. Comparison of relative post-fire bond strength of CFST columns [21, 22] with room temperature specimens

It can be seen that for higher temperatures and older ages of concrete, rectangular specimens exhibited a relatively higher rate of increase in bond strength in comparison with room temperature. Around a 35% increase was observed for rectangular specimens in relation to room-temperature RCFSSST columns. The combined effect of concrete age and high temperature had a positive influence on the relative increase in bond capacity of RCFSSST columns. In addition to hoop stresses in circular CFST columns, micro-locking and chemical adhesion mechanisms govern the bond capacity in circular and square CFST columns [3]. As the temperature increases, the chemical bond between stainless steel and concrete breaks. Hence, the influence of these parameters deteriorates. However, in rectangular CFSST columns, bond capacity is mostly governed by macro-locking mechanisms [5], and hence lower temperatures have little influence on the bond capacity of RCFSSST columns. A summary of the experimental results is shown in Figure 22.

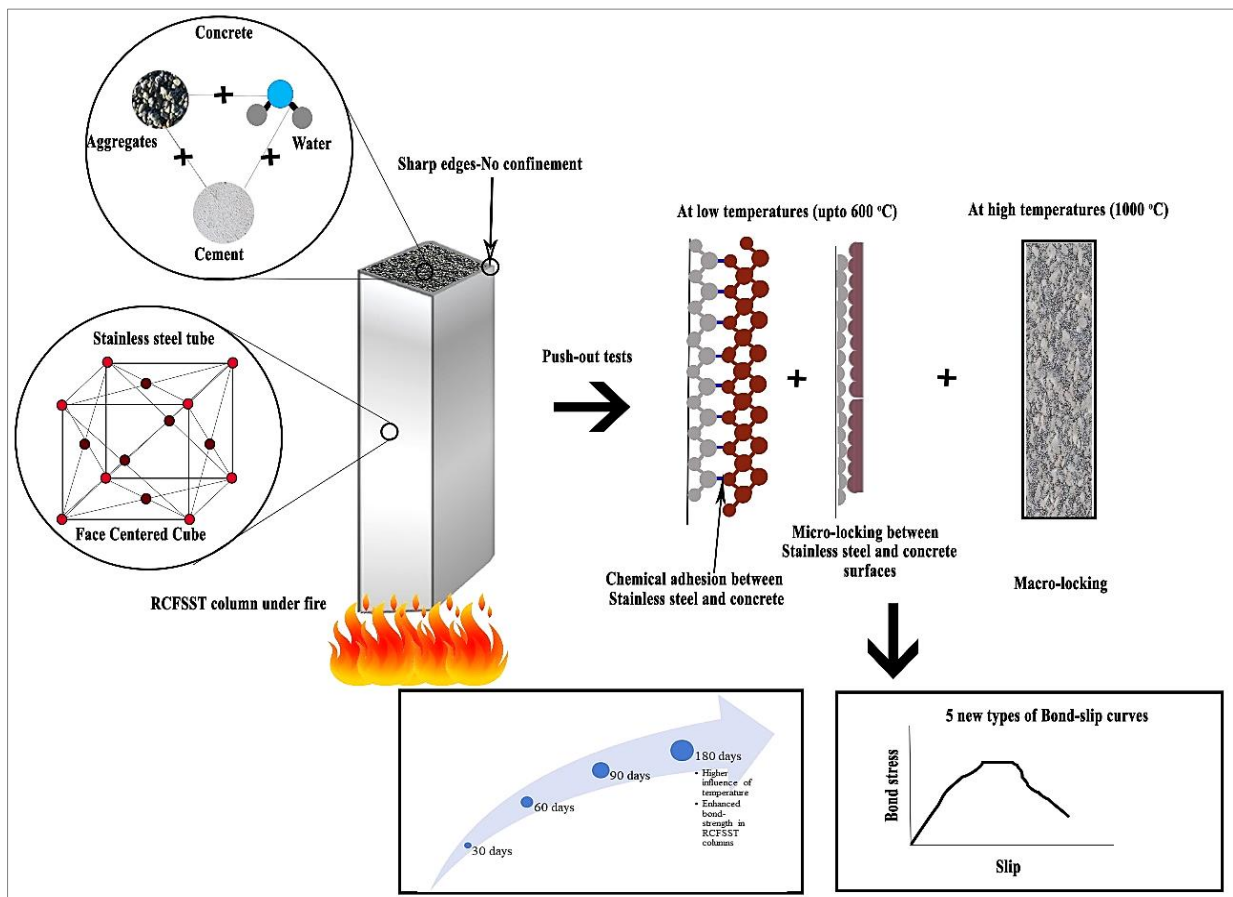


Figure 22. Summary of the experimental results

5. Conclusions

An experimental investigation on the bond strength of rectangular concrete-filled steel tubular columns after fire exposure has been carried out, and the following conclusions were observed:

- Post-fire push-out tests on rectangular CFSST columns were carried out, and the results were compared with existing literature. Push-out tests on ambient temperature test specimens indicate that the rectangular stainless steel tubular columns exhibited lower bond strength than other shapes reported in the literature. Despite this, the bond between rectangular stainless steel and the core concrete significantly increases as the concrete ages.
- It is noted that after exposure to heating and cooling, the bond between the rectangular stainless-steel tube and the core concrete was intact even at earlier concrete ages, and as the concrete aged, the bond strength had substantial growth even under higher temperatures. It is also worth noting that the post-fire test specimens displayed higher resistance against slip during the loading stage of the test. As the concrete ages, this resistance increases to an appreciable extent.
- The test results indicate that high temperatures had a lesser influence on bond strength when compared to the influence of concrete age. For the same concrete age, a rise in temperature resulted in a minor increase in bond strength. However, beyond the recrystallization temperature, the bond strength gradually declined for Type A specimens. When the specimens were cured for around 180 days., i.e., for Type B specimens, elevated temperature had a substantial influence on the bond strength of rectangular CFSST specimens.
- Based on the obtained τ -s results, five types of τ -s curves were observed, each with distinct curve characteristics. Most of the test specimens fall under the type 1 curve, which displayed a three-stage τ -s curve, followed by the type 5 curve with an increase in bond stress beyond the inflection point. It can be concluded that the post-fire bond between the rectangular stainless-steel tube and concrete core displayed appreciable strength at later stages of curing. Other shapes, such as circular or elliptical CFST columns, displayed similar strength at a much earlier concrete age.

It is evident from the τ -s curve that macro-locking was the principal contributing factor for the development of bond strength in RCFSSST columns under the post-fire scenario at older ages of concrete infill. At lower concrete ages, chemical adhesion and micro-locking played a pivotal role in governing the bond strength of RCFSSST columns under post-fire.

6. Declarations

6.1. Author Contributions

Conceptualization, A.K. and A.S.S.; methodology, A.K.; formal analysis, A.K.; investigation, A.K.; resources, A.S.S.; data curation, A.K.; writing—original draft preparation, A.K.; writing—review and editing, A.S.S.; supervision, A.S.S.; project administration, A.S.S. All authors have read and agreed to the published version of the manuscript.

6.2. Data Availability Statement

The data presented in this study are available in the article.

6.3. Funding

The authors received no financial support for the research, authorship, and/or publication of this article.

6.4. Conflicts of Interest

The authors declare no conflict of interest.

7. References

- [1] Liao, F.-Y., Han, L.-H., Tao, Z., & Rasmussen, K. J. R. (2017). Experimental Behavior of Concrete-Filled Stainless Steel Tubular Columns under Cyclic Lateral Loading. *Journal of Structural Engineering*, 143(4), 1–15. doi:10.1061/(asce)st.1943-541x.0001705.
- [2] Yousuf, M., Uy, B., Tao, Z., Remennikov, A., & Liew, J. Y. R. (2013). Transverse impact resistance of hollow and concrete filled stainless steel columns. *Journal of Constructional Steel Research*, 82, 177–189. doi:10.1016/j.jcsr.2013.01.005.
- [3] Chen, Y., Feng, R., Shao, Y., & Zhang, X. (2017). Bond-slip behaviour of concrete-filled stainless steel circular hollow section tubes. *Journal of Constructional Steel Research*, 130, 248–263. doi:10.1016/j.jcsr.2016.12.012.
- [4] Qu, X., Chen, Z., Nethercot, D. A., Gardner, L., & Theofanous, M. (2015). Push-out tests and bond strength of rectangular CFST columns. *Steel and Composite Structures*, 19(1), 21–41. doi:10.12989/scs.2015.19.1.021.

- [5] Song, T.-Y., Tao, Z., Han, L.-H., & Uy, B. (2017). Bond Behavior of Concrete-Filled Steel Tubes at Elevated Temperatures. *Journal of Structural Engineering*, 143(11), 1–12. doi:10.1061/(asce)st.1943-541x.0001890.
- [6] Lakshmanan, S., & Subramanian, N. (2005). Development length of reinforcing bars - Need to revise Indian Codai Provisions. *Indian Concrete Journal*, 79(10), 22.
- [7] Mouli, M., & Khelafi, H. (2007). Strength of short composite rectangular hollow section columns filled with lightweight aggregate concrete. *Engineering Structures*, 29(8), 1791–1797. doi:10.1016/j.engstruct.2006.10.003.
- [8] Xie, K., Huang, K., Huang, L., & Zhu, T. (2023). Experimental study of bond behavior between concrete-filled steel tube and UHPC-encased. *Construction and Building Materials*, 409, 134016. doi:10.1016/j.conbuildmat.2023.134016.
- [9] Xu, T., Bian, X., Liu, Z., Yang, J., & Zhang, Z. (2023). Local bond stress–slip relationship of ribbed reinforcing bars embedded in UHPC: Experiment, modeling, and verification. *Journal of Building Engineering*, 68, 106122. doi:10.1016/j.job.2023.106122.
- [10] Tao, Z., Song, T.-Y., Uy, B., & Han, L.-H. (2016). Bond behavior in concrete-filled steel tubes. *Journal of Constructional Steel Research*, 120, 81–93. doi:10.1016/j.jcsr.2015.12.030.
- [11] Tao, Z., Han, L. H., Uy, B., & Chen, X. (2011). Post-fire bond between the steel tube and concrete in concrete-filled steel tubular columns. *Journal of Constructional Steel Research*, 67(3), 484–496. doi:10.1016/j.jcsr.2010.09.006.
- [12] Feng, R., Chen, Y., He, K., Wei, J., Chen, B., & Zhang, X. (2018). Push-out tests of concrete-filled stainless steel SHS tubes. *Journal of Constructional Steel Research*, 145, 58–69. doi:10.1016/j.jcsr.2018.02.016.
- [13] Guan, M., Lai, Z., Xiao, Q., Du, H., & Zhang, K. (2019). Bond behavior of concrete-filled steel tube columns using manufactured sand (MS-CFT). *Engineering Structures*, 187, 199–208. doi:10.1016/j.engstruct.2019.02.054.
- [14] Lu, Y., Liu, Z., Li, S., & Li, N. (2018). Bond behavior of steel fibers reinforced self-stressing and self-compacting concrete filled steel tube columns. *Construction and Building Materials*, 158, 894–909. doi:10.1016/j.conbuildmat.2017.10.085.
- [15] Wang, L., Chen, H., Zhong, J., Chen, H., Xuan, W., Mi, S., & Yang, H. (2018). Study on the Bond-Slip Performance of CFSSTs Based on Push-Out Tests. *Advances in Materials Science and Engineering*, 2018, 1–13. doi:10.1155/2018/2959827.
- [16] Chen, Z., Tang, J., Zhou, X., Zhou, J., & Chen, J. (2020). Interfacial bond behavior of high strength concrete filled steel tube after exposure to elevated temperatures and cooled by fire hydrant. *Materials*, 13(1). doi:10.3390/ma13010150.
- [17] Almasaeid, H. H., Salman, D. G., Abendeh, R. M., Allouzi, R. A., & Rabayah, H. S. (2024). Interfacial bond capacity prediction of concrete-filled steel tubes utilizing artificial neural network. *Cogent Engineering*, 11(1), 2297501. doi:10.1080/23311916.2023.2297501.
- [18] Guo, Y.-L., Geng, Y., Richard Liew, J. Y., Wang, Y.-Y., & Hong, Z.-H. (2023). Compressive behaviour of circular steel tube confined reinforced concrete (STCRC) columns considering shrinkage and creep. *Thin-Walled Structures*, 192, 111127. doi:10.1016/j.tws.2023.111127.
- [19] Zhang, J., Meng, X., Song, J., Cao, X., & Ma, K. (2023). Push-out tests of interfacial bond slip between H-shaped steel and ultra-high performance concrete. *Structures*, 57, 105268. doi:10.1016/j.istruc.2023.105268.
- [20] Chen, Z., Jia, H., & Li, S. (2022). Bond behavior of recycled aggregate concrete-filled steel tube after elevated temperatures. *Construction and Building Materials*, 325, 126683. doi:10.1016/j.conbuildmat.2022.126683.
- [21] Bahrami, A., & Nematzadeh, M. (2021). Bond behavior of lightweight concrete-filled steel tubes containing rock wool waste after exposure to high temperatures. *Construction and Building Materials*, 300, 124039. doi:10.1016/j.conbuildmat.2021.124039.
- [22] Song, T. Y., Wang, C. H., Liu, X. L., Xiang, K., & Zhou, H. (2023). Post-fire bond behaviour in elliptical concrete filled steel tubes: Experiment and simulation. *Journal of Constructional Steel Research*, 201, 107725. doi:10.1016/j.jcsr.2022.107725.
- [23] Zhao, H., Li, J., Wang, R., Lam, D., & Zhang, Y. (2021). Study on interfacial bond behavior of recycled aggregate concrete filled stainless steel tubes (RAC-FSST). *Construction and Building Materials*, 313, 125532. doi:10.1016/j.conbuildmat.2021.125532.
- [24] Dai, P., Yang, L., Wang, J., Lin, M., & Fan, J. (2022). Bond stress-slip relationship in concrete-filled square stainless steel tubes. *Construction and Building Materials*, 326, 127001. doi:10.1016/j.conbuildmat.2022.127001.
- [25] Parsa-Sharif, M., Nematzadeh, M., & Bahrami, A. (2023). Post-fire load-reversed push-out performance of normal and lightweight concrete-filled steel tube columns: Experiments and predictions. *Structures*, 51, 1414–1437. doi:10.1016/j.istruc.2023.03.091.
- [26] Li, W., Chen, B., Han, L. H., & Packer, J. A. (2022). Pushout tests for concrete-filled double skin steel tubes after exposure to fire. *Thin-Walled Structures*, 176, 109274. doi:10.1016/j.tws.2022.109274.
- [27] Han, L. H., Chen, F., Liao, F. Y., Tao, Z., & Uy, B. (2013). Fire performance of concrete filled stainless steel tubular columns. *Engineering Structures*, 56, 165–181. doi:10.1016/j.engstruct.2013.05.005.

- [28] Ergün, A., Kürklü, G., Serhat Başpınar, M., & Mansour, M. Y. (2013). The effect of cement dosage on mechanical properties of concrete exposed to high temperatures. *Fire Safety Journal*, 55, 160–167. doi:10.1016/j.firesaf.2012.10.016.
- [29] Chan, Y. N., Peng, G. F., & Anson, M. (1999). Residual strength and pore structure of high-strength concrete and normal strength concrete after exposure to high temperatures. *Cement and Concrete Composites*, 21(1), 23–27. doi:10.1016/S0958-9465(98)00034-1.
- [30] Gardner, L., Insausti, A., Ng, K. T., & Ashraf, M. (2010). Elevated temperature material properties of stainless steel alloys. *Journal of Constructional Steel Research*, 66(5), 634–647. doi:10.1016/j.jcsr.2009.12.016.
- [31] Kosmač, A. (2012). *Stainless steels at high temperatures*. Material and Applications Series, Euro Inox, Brussels, Belgium.
- [32] Wang, F.-C., Xie, W.-Q., Li, B., & Han, L.-H. (2022). Experimental study and design of bond behavior in concrete-filled steel tubes (CFST). *Engineering Structures*, 268, 114750. doi:10.1016/j.engstruct.2022.114750.
- [33] Dai, P., Yang, L., Wang, J., Fan, J., & Lin, M. (2021). Experimental study on the steel–concrete bond behaviour of circular concrete-filled stainless steel tubes. *Thin-Walled Structures*, 169, 108506. doi:10.1016/j.tws.2021.108506.